

UV Diagnostics of the Interaction between Starburst Galaxies and the Intergalactic Medium

Crystal L. Martin¹

Space Telescope Science Institute, Baltimore, MD 21218

Abstract. Both galaxies and the intergalactic medium evolve dramatically between $z \approx 2$ and the present. These changes are coupled via galactic winds, cloud accretion, and ionizing radiation. Measurements of these interactions are critical for building a physical understanding of galaxy assembly. This paper reviews the role of starburst galaxies in heating, enriching, and ionizing the intergalactic medium. The strategies used to address these problems rely heavily on access to the rest-frame ultraviolet (UV) spectrum. Rather modest gains in UV sensitivity are shown to produce enormous gains in our ability to follow the very low-density gas dispersed by galactic winds and galaxy interactions. This leverage results from the sensitivity of absorption lines to low ionic columns and the very steep rise in the areal density of quasars toward fainter magnitudes.

1. Introduction – The Assembly of Galaxies

Deep imaging with the Hubble Space Telescope (HST) has been an important catalyst for measuring the cosmic star formation history (Madau et al. 1996). Although corrections for extinction remain controversial, the basic results support predictions for the hierarchical growth of galaxies remarkably well (Baugh, Cole, Frenk, & Lacey 1998 and references therein). The star formation history alone, however, is hardly a sufficient test of this paradigm. One needs to measure the assembly of mass, the dispersal of metals, and the evolution of the angular momentum in galaxies.

To build this physical understanding of galaxy evolution, spectra of thousands of galaxies will be obtained with 6-10 m ground-based telescopes and the Next Generation Space Telescope (NGST). Infrared spectra of galaxies at redshifts $z \geq 0.5$ will contain strong rest-frame-optical emission lines. Star formation rates, metal abundances, and rotation curves will be derived using the same diagnostics developed for nearby galaxies. To avoid the airglow lines of the night sky, many ground-based spectra of $z \geq 1$ galaxies will be obtained at optical wavelengths, and interpretation will rely on diagnostics in the less familiar ultraviolet spectral domain.

The evolution of galaxies cannot be separated, however, from the evolution of the intergalactic medium (IGM). In particular, gas inflow and outflow from

¹Hubble Fellow

galaxies affects the reservoir available for star formation. Metals ejected into the IGM should be counted when computing the integral of the star formation rate over cosmic time. And starburst galaxies may play a role in the ionization of the IGM. Even at the present epoch, galaxies are not thought to be the primary reservoir of baryons (e.g., Cen & Ostriker 1998), so their interaction with this encompassing environment is clearly of fundamental interest for their origin, structure, and evolution.

This paper reviews the role of ultraviolet spectroscopy in building an understanding of galaxy formation and evolution. Applications directly related to the starburst – IGM interaction are emphasized, and the required sensitivity is explored. Relatively little will be said about important applications to the stellar population and dust content of galaxies.

2. UV Spectral Diagnostics

Starburst galaxies have intrinsically blue spectral energy distributions. The Lyman break at 912 Å is the strongest continuum feature in the entire spectral energy distribution (SED). Most of the resonance lines of common ions also lie in the ultraviolet spectral domain. The absorption and emission lines in starburst spectra have three distinct origins: stellar photospheres, stellar winds, and the interstellar medium/halo (Gonzalez-Delgado et al. 1998) and are sensitive probes of the ISM/halo over a wide range of ionization states. Measurements of ion columns and velocity dispersions are not limited to star-forming regions.

2.1. Continuum Emission

Figure 1. Starburst oxygen abundance by number (the solar value is 8.93) vs. the spectral slope in the UV, where $F_\lambda \propto \lambda^\beta$ (Heckman et al. 1998).

The International Ultraviolet Explorer satellite obtained spectra of over 100 nearby, star-forming galaxies (Kinney et al. 1993). Figure 1 shows that the spectral index of the starburst SED, $F_\lambda \propto \lambda^\beta$, is systematically redder in higher metallicity galaxies (Heckman et al. 1998). In metal-rich, dusty starbursts, the stellar continuum is intrinsically blue, but much of the UV is absorbed and

reradiated at longer wavelengths. The continua of metal-poor galaxies in the local universe do remain quite blue. Figure 1 shows that the observed spectral index approaches the intrinsic value $\beta \sim -2$ in galaxies with $\log O/H \approx -4$. Many of these dwarf galaxies are young and only a small fraction of their total gas mass has been turned into stars.

The oldest stars in the universe, some of which might have formed in very early starbursts, are also studied in the UV spectral domain. The continuum radiation from E galaxies and bulges of spiral galaxies plummets around 4000 Å, but shows a strong upturn shortward of 2700 Å (Bertola et al. 1982, Figure 1) due to horizontal branch stars. In nearby galaxies, this population may be resolved with HST/STIS. Post extreme horizontal branch stars, a small fraction of the population, have been resolved in M32 and M31 with HST/FOC (Brown et al. 1998).

2.2. Starburst Sightlines

Spectra with HST/GHRS of UV-bright star clusters in several galaxies were obtained (Kunth et al. 1998; Heckman & Leitherer 1997). The narrow, low-ionization lines arise from absorption in the ISM of these starburst galaxies and are sometimes blueshifted with respect to the photospheric lines. Figure 2 shows Si II and Si III absorption in NGC 1705, a postburst dwarf galaxy, at a velocity 100 km s⁻¹ less than the photospheric C III absorption. The optical emission-line radiation splits into two components, redshifted and blueshifted by similar amounts (Meurer et al. 1992). The UV measurements confirm that this shell of gas is expanding, rather than infalling and show that a cooler gas phase is participating in the outflow.

Figure 2. HST GHRS spectrum of a dwarf starburst galaxy NGC 1705 from the study of Heckman & Leitherer (1997).

The interstellar absorption lines in NGC 1705 are wider than the corresponding Galactic absorption lines. The intrinsic width, ~ 120 km s⁻¹, probably represents the macroscopic motion of the absorbing clouds. In general, the broadening of interstellar lines, unlike stellar wind lines, is not directly correlated with the ionic column (Heckman et al. 1998). The width seems to be more

closely related to the strength of the burst and the total mechanical energy available.

Higher resolution GHR spectra show Ly α in emission in 4 of 8 H II galaxies with blueshifted interstellar absorption lines (Kunth et al. 1998). Although Ly α is expected to be produced in abundance, virtually none is expected to escape a static, homogeneous medium. Resonant scattering of the Ly α photons greatly increases the probability for absorption by dust in a static medium (Charlot & Fall 1991). However, since the cross section drops abruptly longward of the resonance, Ly α backscattered from the receding side of an expanding H I shell could escape (Ahn & Lee 1998). Indeed, Kunth et al. suggest that the detected emission is redshifted and find Ly α absorption below the systemic velocity – i.e. a P Cygni-like line profile. The velocity structure of the ISM seems to be a very important factor for determining the detectability of Ly α emission.

A typical high-redshift, Lyman break galaxy shows relatively weak stellar wind lines, blueshifted lines from ions in lower ionization states, and a P-Cygni-like Ly α profile (Lowenthal et al. 1997). Outflows could therefore be prevalent in high-redshift galaxies. However, deriving their properties from these line measurements clearly requires a local calibration.

2.3. Halo Sightlines

Galactic winds must be transient phenomena. Starbursts last of order 10 Myr, and the supernova rate plummets after 40 Myr. Following the ejected material well beyond the stage where it is illuminated by the starburst is critical for determining its fate. Absorption-line studies using QSO sightlines are the best way to follow this material with low column density and unknown ionization state. They also provide a means to measure the rotational speed of the neutral medium at column densities several orders of magnitude below the $\sim 10^{19}$ cm $^{-2}$ limit of 21-cm emission. Such constraints on the extent of the dark matter halo are needed to constrain models of the escape velocity. Few sightlines are currently accessible, although two bright quasars are projected near the starburst galaxy NGC 520. At a separation of $24h^{-1}$ kpc, Mg II absorption is detected; and a possible detection at $53h^{-1}$ kpc is reported (Norman et al. 1996).

Testing all galaxies for the presence of absorbing halos would provide an important link to the ISM in high redshift galaxies. In QSO spectra, Mg II $\lambda\lambda 2796, 2803$ absorption lines at $0.2 < z < 1$ are associated with galaxies at separations $< 40h^{-1}$ kpc from the sightline (Steidel et al. 1994). Equivalent widths, $W_\lambda > 0.3$ Å, correspond to $N_{\text{HI}} \geq 2 \times 10^{17}$ cm $^{-2}$. Sightlines through disks and halos of nearby galaxies typically show no absorption at separations $\geq 31h^{-1}$ kpc to even higher sensitivities, $W_{\lambda 2796} = 0.04$ to 0.09 Å (Bowen et al. 1995). Figure 3 illustrates how similar these results are. The sharp cutoff could

be an ionization effect since Mg II disappears as the H I becomes optically thin at the Lyman limit (Steidel & Sargent 1992).

Figure 3. Separation of QSO sightline versus galactic magnitude from the study of Bowen, Blades, & Pettini (1995). Filled symbols represent detections of Mg II absorption. The dashed line represents the gas cross section in moderate redshift galaxies.

2.4. Metal Enrichment

The metallicity of star-forming galaxies has typically been derived from the emission-line ratios of H II regions. Although their optical spectra contain prominent lines of O, N, and S, access to the ultraviolet spectrum is required to measure the C abundance. The C/O ratio, typically $C\text{ III}] \lambda 1909 / [O\text{ III}] \lambda 5007$, provides a measure of the time elapsed since the last burst. The stars producing most of the C live much longer than those synthesizing O. The relatively high ratio of C/O in I Zw18, for example, has been used to argue that some stars formed in this notoriously oxygen-poor galaxy prior to the current burst (Garnett et al. 1997). For higher redshift galaxies, more closely spaced lines would provide a more accessible pollution index. Initial efforts to calibrate the $C\text{ II}] 2326$ to $[O\text{ II}] 3727,29$ ratio as a measure of the C/O ratio show promise, but C measurements are needed for more local galaxies (Kobulnicky & Skillman 1998).

Ultraviolet absorption-line studies are potentially a sensitive probe of abundance ratios. The equivalent width of stellar-wind lines may be a good metallicity indicator (Heckman et al. 1998). Interstellar absorption provides an unique opportunity to measure abundance ratios in infalling gas, tidal ejecta, and galactic winds. But sightlines toward the starburst region typically have high H I column densities, and many interstellar lines are optically thick (Heckman et al.

1998) and insensitive to abundance (Fig. 4). Little has been done conclusively at current sensitivities (Pettini & Lipman 1995).

Figure 4. Theoretical fits to the O I λ 1302 profile of I Zw 18 as shown by Pettini and Lipman (1995).

2.5. Do Ionizing Photons Escape from Galaxies?

Starburst galaxies could be substantial contributors to the metagalactic ionizing radiation field at $z \geq 3$ (Miralda-Escudé & Ostriker 1990; Madau & Shull 1996). The observational evidence for escaping Lyman continuum radiation is not yet definitive, however. An H I column of only $1.6 \times 10^{17} \text{ cm}^{-2}$ is sufficient to absorb a 1 Rydberg photon. Yet, in nearby galaxies H α emission from recombining gas is seen at distances ~ 1 kpc from H II regions; and the spectral gradient is often consistent with the dilution of photons leaking out of H II complexes (Martin 1997). This large propagation distance must be closely connected to the geometry of the ISM (Dove & Shull 1994). The excitation mechanism at many times this distance, where extremely low surface brightness H α emission

has been detected, will not be determined unambiguously until spectra can be obtained (Tufté & Reynolds 1998; Bland-Hawthorn et al. 1997).

Figure 5. Total number of Lyman continuum photons vs luminosity at 900 Å for three starburst models from the study of Leitherer et al. 1995.

Measurement of the Lyman continuum flux shortward of the Lyman limit is a more direct approach. The recombination rate measured from the Balmer lines puts a lower limit on the production rate of ionizing photons. The ratio of this production rate to the luminosity density at 900 Å is relatively insensitive to the starburst parameters as illustrated in Figure 5. Upper limits on L_{λ}^{900} therefore provide upper limits on the escape fraction. The limits derived from HUT spectra of 4 nearby starbursts range from 3% (Leitherer et al. 1995) to as much as 57% (Hurwitz et al. 1997). The difference arises from the treatment of the complex gas-phase absorption of the Milky Way.

3. Science Drivers

Measurements of ionic columns and the Lyman break are critical for understanding the impact of starburst galaxies on the IGM and the influence of environment on the starburst phenomenon. These types of studies require access to the ultraviolet spectral domain. To answer questions pertaining to the ubiquity of halos, hundreds of galaxies should be probed. Since the gas may not recombine as fast as it cools, higher ionization states need to be probed as well as those in the H I medium. The most serious limitation to the interpretation is the ambiguity between absorption from relict winds and tidally stripped gas. Access to large samples of galaxies and multiple sightlines per galaxy are needed will resolve this issue. In this section, I discuss the limits of absorption-line studies with the HST instruments STIS and COS; sensitivity to the Lyman-break is compared at several redshifts. The goal is to determine how large a change in sensitivity would be required to enable a new genre of research programs in this area.

3.1. Availability of Sightlines

Absorption lines are only powerful probes if bright quasars, star clusters, gamma ray bursts, supernovae, etc. can be found sufficiently close to the galaxy under study. Star clusters have several disadvantages. Studies are limited to the subset of starburst galaxies with low reddening, and absorption from the ISM in the starburst region can be confused with that from an extended halo. Quasar sightlines provide unambiguous probes of the extended halo. Figure 6 illustrates the growth in the number of quasars per square degree toward fainter magnitude. A rather modest gain in sensitivity, factor of 2.8, provides access to an order of magnitude more sightlines!

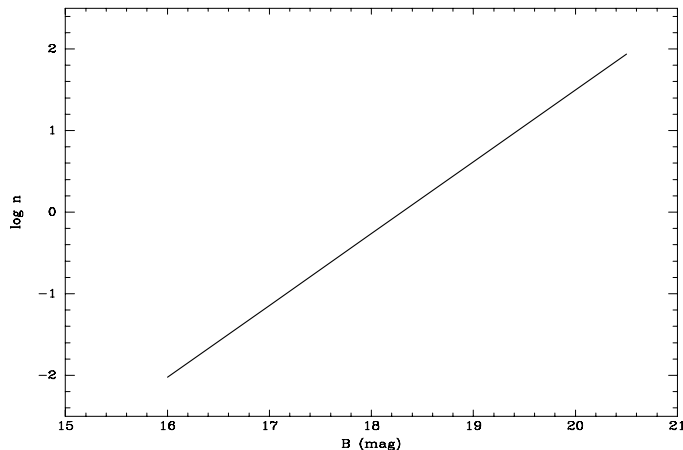


Figure 6. Number of QSOs per unit area vs apparent magnitude based on model of Weedman (1986).

Most of the moderate-redshift metal line systems have been associated with bright, $L \sim L^*$, galaxies. When fainter galaxies are detected the separation from the sightline tends to be lower (Steidel 1995; Chen et al. 1998). Since material is clearly being ejected from some dwarf galaxies, the lack of dwarf galaxy absorption line systems is quite interesting (McLin, Giroux, & Stocke 1998). Suppose gas streams out of a ruptured superbubble at the sound speed, $\sim 300 \text{ km s}^{-1}$. Between bursts, perhaps a few hundred Myr, debris would have spread to distances of $\sim 50 \text{ kpc}$. Estimates of the mass lost in these events are of the order of the mass turned into stars, or roughly $\sim 10^6 M_\odot$. The average column density through this wind relic is then only $N_H \approx 1.6 \times 10^{16} (M/10^6 M_\odot)(50 \text{ kpc}/R)^2$.

Table 1 illustrates the equivalent widths of several strong lines. An H I column of 10^{16} cm^{-2} , metallicity 1/3 solar, and solar abundance ratios were assumed. Regardless of whether the halo is mainly neutral H or highly ionized, the strongest lines would only be a few mÅ wide, where $W_\lambda \propto N_i \lambda^2 f$. The equivalent width determines the S/N ratio that must be reached in the QSO continuum. Assuming that the continuum level itself is well-known, the S/N of the integral over N resolution elements is $S/N = \sqrt{N} \lambda / (R \delta W_\lambda)$, where R is the spectral resolution $\lambda/\Delta\lambda$. Resolutions of 10-30 km s^{-1} will probably be

necessary to begin to resolve these lines. Integrating over 1 to 10 resolution elements at $R = 10,000$ to $30,000$, the S/N must be several hundred to detect metal lines from gas columns of order 10^{16} cm^{-2} . Higher columns like those detected at moderate redshift can be found with $S/N \sim 30$.

Table 1
Detecting Metals in $N_{\text{HI}} = 10^{16} \text{ cm}^{-2}$ ($1/3 Z_{\odot}$)

| Ion | $W_{\lambda}(10^{16})$ Å | S/N 5σ |
|--------------|-----------------------------|--------------------|
| Mg II 2796.3 | 0.0054 | 270 |
| Si II 1263.3 | 0.0017 | 400 |
| C II 1334.5 | 0.0024 | 290 |
| C IV 1549.1 | 0.0073 | 110 |
| S iIV 1396.3 | 0.0016 | 460 |
| O VI 1033.8 | 0.0053 | 100 |

Table 2
Limiting QSO B Magnitude at $\sim 15 \text{ km s}^{-1}$ Resolution^a

| Exp Time | S/N | 10^4 s | 10^5 | 10^6 s |
|------------|-------|------------------|--------|------------------|
| STIS G230M | 30 | 14.6 | 16.9 | 18.6 |
| COS G260M | 30 | 14.4 | 16.9 | 19.4 |
| STIS G140M | 30 | 14.8 | 17.3 | 19.8 |
| COS G160M | 30 | 14.0 | 16.5 | 19.0 |
| STIS G230M | 300 | 9.8 | 12.3 | 14.8 |
| STIS G140M | 300 | 9.8 | 12.3 | 14.8 |
| SUVO? | 30 | 20 | 22.5 | 25 |
| SUVO? | 300 | 15 | 17.5 | 20 |

^a An observed spectral energy distribution with $F_{\lambda} \propto \lambda^{-1}$ was assumed. In practice the maximum achievable S/N ratio may be limited by the exposure and stability of the flatfields.

Table 2 illustrates the quasar B magnitude that can be reached with the current and planned instruments on HST. The three exposure-time columns represent practical limits for: (1) a survey project; (2) a special target; and (3) a campaign like the Hubble Deep Field. Sensitivities for STIS were taken from the instrument handbook and the on-line exposure time calculator. The estimates for COS assume that $S/N = 10$ will be obtained in 10^4 s at $F_{\lambda} = 1.5 \times 10^{-15} \text{ ergs s}^{-1} \text{ cm}^{-2} \text{ \AA}^{-1}$. Over a single line, the gain with COS is not dramatic; but COS provides about 6 times more spectral coverage per tilt at this resolution. At low S/N , the detector noise limits the depth reached with STIS in the near-UV, so COS will provide a dramatic gain.

If detector noise is negligible, then the number of potential sightlines increases by a factor of ~ 160 with each successive column to the right. At $B = 18$, the average area on the sky per quasar is about 2 square degrees. However, because the counts rise so steeply with magnitude, one could obtain

a sightline per galaxy, about $10' \times 10'$, if $B = 20$ were accessible. Indeed, STIS could reach $B \approx 19.8$ in a dedicated HDF-like campaign. To complete the type of statistical study called for, however, one would like data for perhaps 5 sightlines towards 200 galaxies. Without some type of multiplexing, this program would take $\sim 10^9$ s to complete with current and planned instruments! Yet with only a factor of 140 gain in sensitivity, surveys for $N_{\text{HI}} \sim 10^{17} \text{ cm}^{-2}$ halos could be completed in a year. Multiplexing could reduce the required gain in sensitivity by a factor of 5. With this type of improvement, Table 2 shows that it also becomes possible to observe selected lines of sight at $S/N=300$ and measure the metallicity in columns with $N_{\text{HI}} \approx 10^{16} \text{ cm}^{-2}$.

3.2. The Dispersal of Metals

Along starburst galaxy sightlines, moderately high S/N is required to measure weaker, unsaturated lines. Pettini & Lipman (1995) suggest that measurements of S II $\lambda\lambda 1250.6, 1253.8, 1259.5$ at $S/N = 10$ could determine whether the H I halo is significantly more metal-poor than the star-forming regions. Measurement of the O column, however, will require either much higher sensitivity to reach O I $\lambda 1355$ or access to O I multiplets shortward of 1190 \AA . It is perhaps worth emphasizing that good velocity resolution, $\sim 10 \text{ km s}^{-1}$, is needed to untangle individual kinematic components which would artificially broaden the lines. Similar techniques will provide important measures of abundances in intergalactic clouds. The sum of metals inside and outside galaxies provide an important check on the integrated cosmic star formation history (Renzini 1997).

3.3. Does Ionizing Radiation Escape from Galaxies?

The contribution of galaxies to the metagalactic ionizing radiation should be measured locally and at high redshift. The escape fraction may be different at various epochs, and the source of systematic uncertainties are different at these epochs. It is also conceivable that the escape fraction would be higher in starbursting dwarf galaxies, so similar measurements must eventually be made for these galaxies. Modeling the gas-phase absorption of the Milky Way near the Lyman limit is complex. In practice, galaxies at $z > 0.03$ are preferred (Hurwitz et al. 1997). At $z = 2.5$, the Lyman break enters the optical domain. At moderate redshifts HST could, in principle, observe the Lyman break; but it is not sensitive below $z = 0.3$ because of the fall-off in system throughput.

Measuring the continuum flux density below the Lyman limit is challenging at any wavelength/redshift. For example, a bursting dwarf galaxy and a star-forming, spiral galaxy would produce H ionizing photons at rates of $Q_H \approx 5 \times 10^{51} \text{ s}^{-1}$ and $Q_H \approx 5 \times 10^{53} \text{ s}^{-1}$, respectively. For these production rates, Figure 7 shows the redshifted flux density just below the Lyman limit. Some starbursts lie above this line. Leitherer et al. (1995) examined four starbursts with $Q_H = 9.5 \times 10^{52} \text{ s}^{-1}$ to $3.6 \times 10^{54} \text{ s}^{-1}$. The rates in some high-redshift Lyman break galaxies are even higher, and a typical 1500 \AA flux density is shown in Figure 7. Note that the solid lines severely overpredict the observed flux density at $z > 3$ where the opacity from intergalactic H I attenuates the flux by an order of magnitude.

Figure 7 clearly shows the advantage of making measurements at 940 \AA to 980 \AA . Even locally though, fluxes about a factor of 10 lower than those reached

with HUT are needed to measure bursting dwarfs. To compare the feasibility at moderate and high-redshift, a common resolution of $\sim 400 \text{ km s}^{-1}$ is used in Figure 7, and a 10^4 sec observation is required to reach a S/N of 10. The points for STIS are based on the G140L and G230L gratings. The relative gain with COS, open symbols, would be dramatic if the comparison was made to the STIS echelle modes; but an extensive spectral range is not required for this problem. The hexagons represent a single 10-m telescope with total system throughputs of 4% and 40%. The figure is overly optimistic about the ease of detecting the continuum in high-redshift galaxies because no intergalactic attenuation is included in the model. However, the star formation rates in some high-redshift starbursts are much larger, possibly factors ~ 100 , than the models shown, so detections are likely to be made first for the high-redshift starbursts.

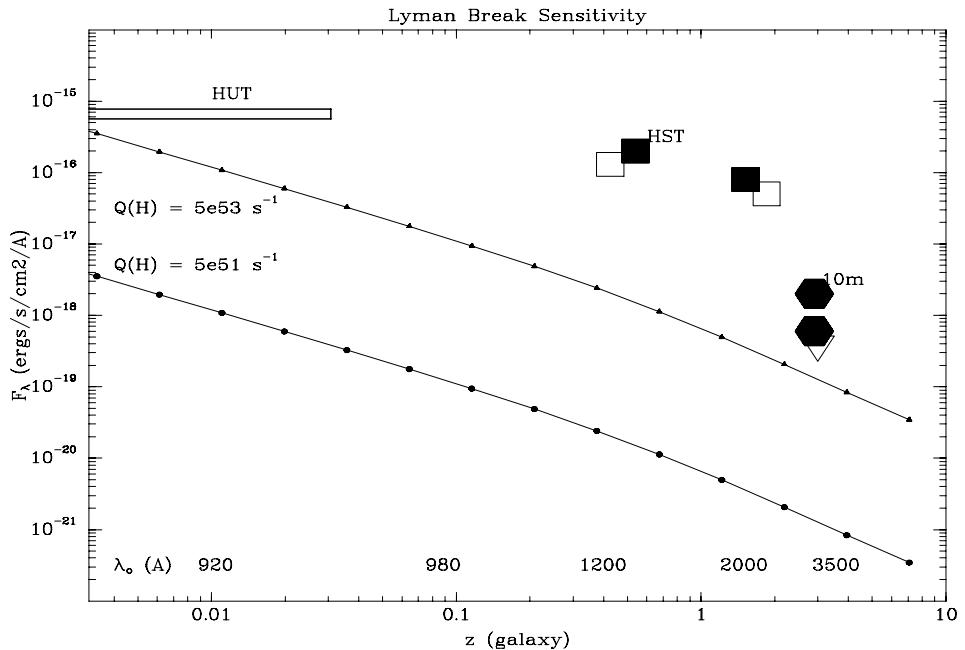


Figure 7. Unattenuated flux density shortward of the Lyman break as a function of the galaxy’s redshift. Curves are shown for a 30-Doradus-like H II region and a star-forming, spiral galaxy. The inverted triangle shows the flux density at 1500 \AA for a typical Lyman break galaxy (Pettini et al. 1997). The large symbols represent the sensitivity levels of particular instruments, see text for details.

4. Conclusions

This paper has drawn attention to several fundamental questions about the impact of starbursts on the surrounding interstellar and intergalactic gas. It should be clear that answering these questions will require UV spectroscopy at resolutions $\geq 10,000$ and sensitivities approximately 140 times higher than those reachable in surveys with HST+STIS or HST+COS. Some type of multiplexing should be considered to obtain spectra of several quasars per galaxy halo simul-

taneously. A strong effort should also be made to determine whether detector sensitivity can be increased by a factor ~ 10 in the UV. With such advances, the aperture of the next space UV observatory need only exceed that of HST by a factor of 3 to provide the opportunity for extraordinary advances.

Acknowledgments. This work was supported by NASA through Hubble Fellowship grant HF-01083.01-96A. It is a pleasure to thank David Bowen, Tim Heckman, Claus Leitherer, Max Pettini, and Daniel Weedman for contributing figures from their work.

References

- Ahn, S. & Lee, H. 1998, astro-ph/9801031.
- Baugh, C. M., Cole, S., Frenk, C. S., & Lacey, C. G. 1998, ApJ, 498, 504.
- Bertola et al. 1982, ApJ, 254, 494.
- Bland-Hawthorn, J., Freeman, K. C., & Quinn, P. J. 1997, ApJ, 490, 143.
- Bowen, D. V., Blades, C. J., & Pettini, M. 1995, ApJ, 448, 634.
- Brown, T. M., Ferguson, H. C., Stanford, S. A., & Deharveng, J.-M. 1998, ApJ, 504, 113.
- Cen, R. & Ostriker, J. P. 1998, to appear in Science
- Charlot, S. & Fall, S. M. 1991, ApJ, 378, 471.
- Dove, J. B. & Shull, J. M. 1994, ApJ, 430, 222.
- Garnett, D. R. et al. 1997, ApJ, 481, 174.
- Gonzalez Delgado, R. M. et al. 1998, ApJ, 495, 698.
- Heckman, T. M. et al. 1998, ApJ, 503, 646.
- Heckman, T. M. & Leitherer, C. 1997, AJ, 114, 69.
- Hurwitz, M., Jelinsky, P., & Dixon, W. 1997, ApJ, 481, L31.
- Kinney, A. L., et al. 1993, ApJS, 86, 5.
- Kobulnicky, H. A. & Skillman, E. D. 1998, ApJ, 497, 601.
- Kunth, D. et al. 1998, A&A, 334, 11.
- Leitherer, C. et al. 1995, ApJ, 454, 19L.
- Lowenthal, J. D. et al. 1997, ApJ, 481, 673.
- Madau, P. et al. 1996, MNRAS, 283, 1388.
- Madau, P. & Shull, J. M. 1996, ApJ, 457, 551.
- Martin, C. L. 1997, ApJ, 491, 561.
- McLin, K. M., Giroux, M. L., & Stocke, J. T. 1998, in Galactic Halos, ed. D. Zaritsky.
- Meurer, G. R. et al. 1992, AJ, 103, 60.
- Miralda-Escudé, J. & Ostriker, J. P. 1990, ApJ, 350, 1.
- Mushotzky, R. F. & Loewenstein, M. 1997, ApJ, 481, L63.
- Norman, C. et al. 1996, ApJ, 472, 73.
- Pettini, M. & Lipman, K. 1995, A&A, 297, L63.

- Pettini, M, et al. 1997, in *Origins*, ASP Conf. Series, Vol. 148, ed. C. E. Woodward, J. M. Shull, & H. A. Thronson, 67
- Renzini, A. 1997, ApJ, 488, 35.
- Steidel, C. C., Dickinson, M., & Persson, S. E. 1994, ApJ, 437, 75.
- Steidel, C. C. & Sargent, 1992, ApJS, 80, 1
- Tufte, S. L., Reynolds, R. J., & Haffner, L. M. 1998, astro-ph/9807157.
- Weedman, D. W. 1986, Quasar Astronomy, (Cambridge University Press, Cambridge).